23

Infrared Carbon Dioxide Sensor Based on Light- and Photodiodes from InAsSb(P) Solid Solutions

 R.E. Kunkov, S.A. Karandashev, A.A. Klimov, T.S. Lukhmyrina, M.A. Remenny

Ioffe Institute,
St. Petersburg, Russia

e-mail: Kunkov.re@mail.ioffe.ru

Received April 30, 2025
Revised August 28, 2025
Accepted October 24, 2025

Results are reported on the development and investigation of light- and photodiodes based on the *n*-InAs/N-InAsSbP/InAsSb/P-InAsSbP heterostructure with an operating wavelength of about 4.2 μm ($T = 296$ K). Data on electroluminescence and photoelectric characteristics in the temperature range 200–500 K are presented. Results are reported on the development of a nondispersive compact carbon dioxide sensor based on the aforementioned components, characterized by a detection threshold of no more than 25 ppm at a sampling frequency of 128 ms, optical path of 2 cm, and power consumption below 50 mW.

Keywords: InAsSb heterostructures, mid-wave IR LEDs, mid-wave IR photodiodes, nondispersive carbon dioxide gas sensor.

DOI: 10.61011/EOS.2025.11.62918.7969-25

Introduction

Carbon dioxide (CO_2) is a daily companion of human life, with negative effects on the human body beginning at concentrations around 0.1–0.15 %vol (1000–1500 ppm), so permissible levels of carbon dioxide in industrial, office, and residential premises are strictly regulated, and the importance of its control is universally recognized.

One of the most promising approaches to creating carbon dioxide sensors is the infrared (IR) nondispersive (Non-dispersive Infrared — NDIR) method, based on selective absorption of IR radiation by gas molecules and characterized by high selectivity to the gas, long service life, and sensitivity down to units of ppm [1]. Obviously, the parameters of the optoelectronic components used largely determine the achievable levels of threshold sensitivity and sensor accuracy. To date, sensors based on thermal IR radiation sources and detectors [2] have gained the widest acceptance, characterized by high power consumption, low speed, and relatively low sensitivity. IR (mid-wave) sensors using photodiodes and optically pumped LEDs based on lead salts [3] are also employed, the disadvantage of which is the lack of long-term stability.

A promising alternative is the development of IR sensors using light- and photodiodes based on A^3B^5 materials, in particular heterostructures from InAsSb(P) solid solutions, characterized by high metallurgical stability and relatively low cost. For many years at the Ioffe Institute RAS, development and research of optoelectronic components based on InAsSb solid solution have been conducted, including those operating at wavelengths around 4.2 μm [4–6], and optical sensors based on them [7]. The objectives of this work were to improve the characteristics of optoelectronic components (light-emitting diodes (LED) and photodiodes (PD) hereafter), enhance the efficiency of their operation as an optopair over a wide temperature range, and develop a compact nondispersive carbon dioxide sensor based on them with a high degree of integration of optical, optoelectronic, and electronic components.

Experimental Results

The investigated light- and photodiode samples were fabricated from the N-InAsSbP/InAsSb$_x$/P-InAsSbP heterostructure with an active/photosensitive region of InAsSb$_x$ ($x = 0.08$) thickness 3–4 μm grown by LPE onn^+-InAs (100) substrates. Characteristic features of the light- and photodiode design were flip-chip construction with an active/photosensitive area diameter of about 140 μm and emission input/output through a 20–40 μm-thick substrate, immersion coupling of the chip with a 3.5 mm diameter Si lens with antireflection coating.

Fig. 1 shows the spectral characteristics of electroluminescence at a pump current of 200 mA in continuous mode and photosensitivity in the temperature range 200–500 K.

Compared to previously published results, the possibility of operation of mid-wave optoelectronic components at such high temperatures (up to 500 K) is demonstrated for the first time, with increased current sensitivity and „dark“ resistance of PD, as well as output power of LED [8]. Improvement of parameters was achieved due to optimization of the epitaxial structure design, in particular by reducing the thickness of the active/photosensitive region, which led to reduced self-absorption of radiation and decreased dark current.

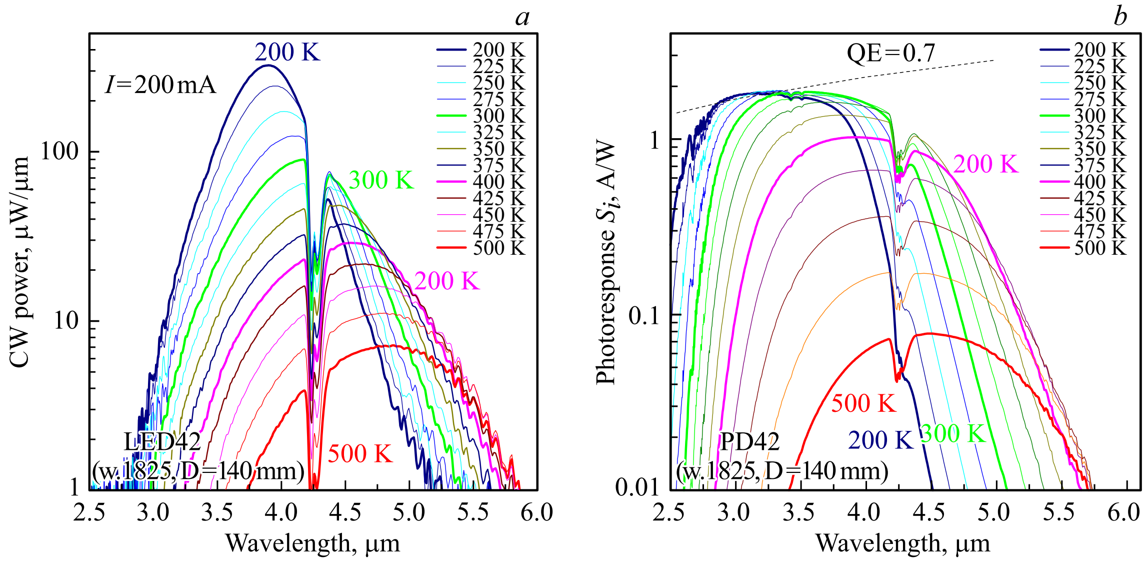

Figure 1. Electroluminescence spectra (a) and current sensitivity (b) in the temperature range 200–500 K.

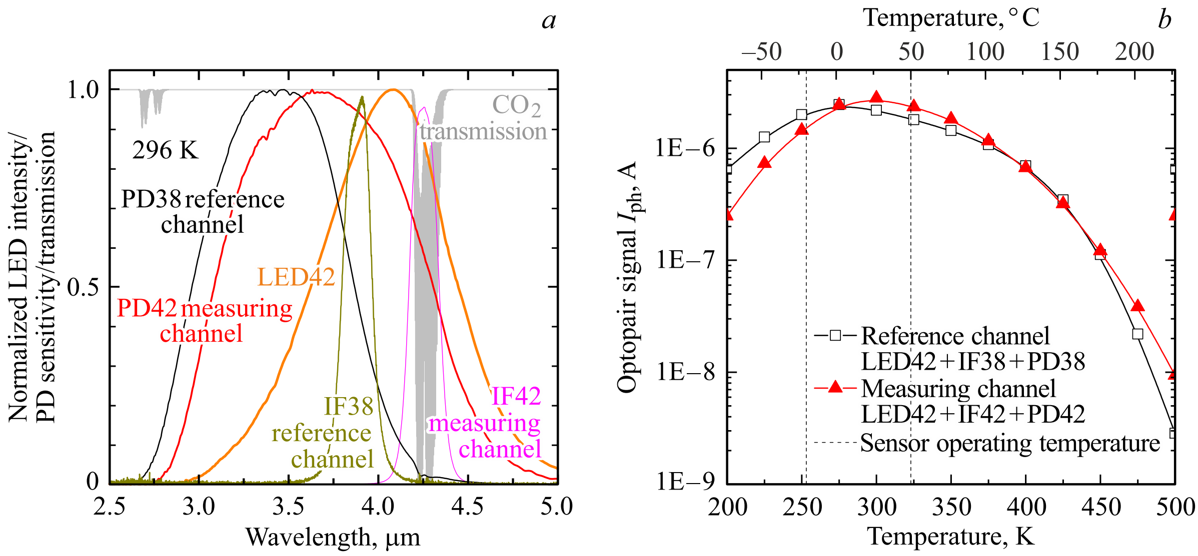

Figure 2. Normalized spectral characteristics of the optoelectronic components used and CO_2 absorption (a); temperature dependences of optopair signals in the measurement and reference channels (b).

Based on the above-described components, as well as a previously developed immersion photodiode with an operating wavelength of 3.8 μm denoted in the figures as PD38, a compact nondispersive optical sensor was developed with the following characteristic features: an optical scheme with measurement and reference channels, in which radiation from the LED (LED42) is split and filtered using interference optical filters (IF42 and IF38) and focused on the measurement (PD42) and reference (PD38) channels. The normalized spectral characteristics of these components at room temperature, as well as the carbon dioxide transmission spectrum in the wavelength range used, are shown in Fig. 2, a. Fig. 2, b presents the temperature dependences of the integral signals of the optopairs in the measurement (LED42-IF42-PD42) and reference (LED42-IF38-PD38) channels, calculated using the formula

$$I_{ph} = \int_{\lambda_1}^{\lambda_2} P_{\mathrm{LED}}(\lambda) T_{\mathrm{IF}x}(\lambda) S_{\mathrm{IPD}x}(\lambda) d\lambda, \qquad (1)$$

where $P_{\mathrm{LED}}(\lambda)$ — spectral dependence of LED42 power, $T_{\mathrm{IF}x}(\lambda)$ — transmission spectrum of the interference filter, $S_{\mathrm{IPD}x}(\lambda)$ — current sensitivity spectrum of the photodiode for the corresponding optopair.

Based on the obtained dependences of „dark“ resistance on temperature (Fig. 3, a), the noises of the photoreceiver

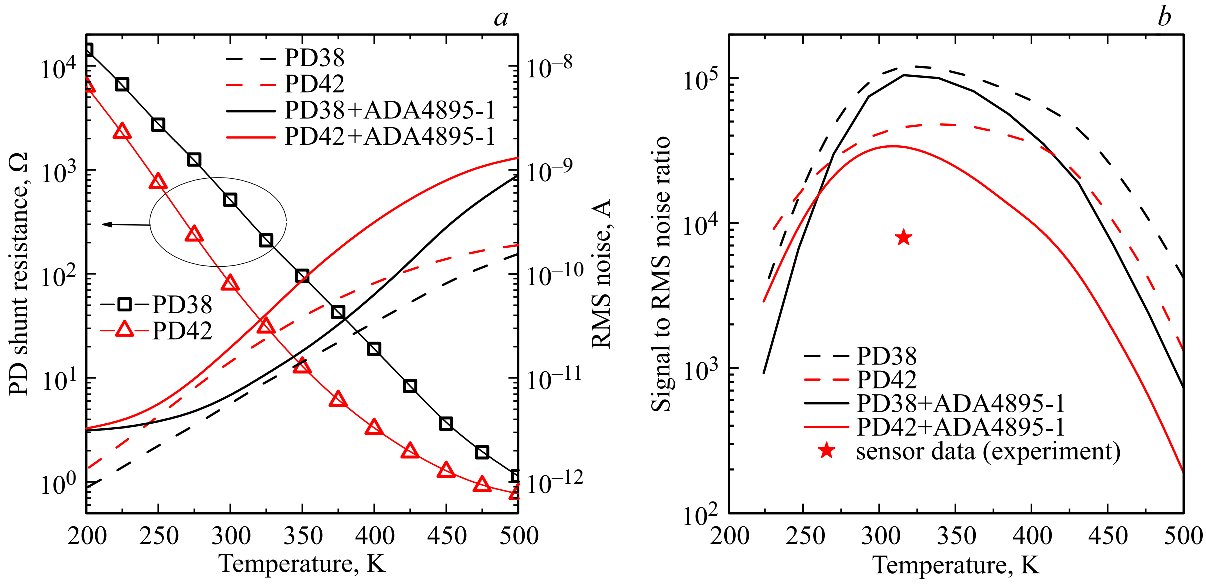

Figure 3. Temperature dependences of dark resistance and noise levels of photodiodes individually and in the op-amp circuit (*a*), signal-to-noise ratios of optopairs (*b*).

individually and together with the first-stage operational amplifier ADA4895-1 were calculated. The calculation was performed for a bandwidth of $\Delta f = 1\,\mathrm{Hz}$ beyond the influence of $1/f$ noises using the formula [9]

$$I_{n\_\Sigma}(\Delta f) = \Delta f \sqrt{i_{n\_PD}^2 + i_{OP}^2 + i_{fb}^2}$$

$$= \Delta f \sqrt{\frac{4kT}{R_o} + i_{n\_OP}^2 + \left(\frac{e_{n\_OP}}{R_o}\right)^2 + \frac{4kT}{R_{fb}}}\ [A], \quad (2)$$

where the first term pertains to photodiode noises, the second and third — operational amplifier (op-amp) noises of the first stage, and the last term — thermal noise of the first-stage feedback resistance. As seen from Fig. 3, *a*, the op-amp makes a significant contribution to the noises, especially at the temperature range boundaries. At elevated temperatures, the main contribution comes from op-amp voltage noises (e_{n_OP}), while at reduced temperatures, it likely approaches the asymptote of thermal noise from the feedback resistance R_{fb}.

Fig. 3, *b* shows the temperature dependences of the signal-to-noise ratio obtained based on the dependences in Figs. 2, *b* and 3, *a*, as well as data for room temperature obtained with the developed carbon dioxide sensor prototype. The lower experimental signal-to-noise ratio value is most likely due to the greater bandwidth of real digital filters and losses from optical system imperfections.

To assess the carbon dioxide detection threshold, the sensor transfer function was calculated at room temperature. For this, using the formula

$$I_{ph} = \int_{\lambda_1}^{\lambda_2} (1 - \exp(-k(\lambda)Cd))P_{\mathrm{LED42}}(\lambda)T_{\mathrm{IF42}}(\lambda)S_{\mathrm{IPD42}}(\lambda)d\lambda \quad (3)$$

($k(\lambda)$ — spectral dependence of the carbon dioxide absorption coefficient, C — gas concentration in %vol, d — optical path length), the integral signals of the optopairs were calculated taking into account the IR transmission spectrum over an optical path of 2 cm. Data for the spectral dependence of the carbon dioxide absorption coefficient were taken from the open HITRAN library.

The obtained dependence is shown in Fig. 4, *a* in ADC counts. From the obtained SNR and sensor transfer function dependences, assuming small change with temperature, the carbon dioxide detection threshold was calculated in the temperature range 200–500 K for a bandwidth of $\Delta f = 1\,\mathrm{Hz}$, with experimental points obtained during prototype testing at room temperature also plotted. The root-mean-square noise (RMS) was estimated at 15 ADC counts when assessing the useful signal amplitude from 85940 to 37127 ADC counts, with the detection threshold at the 2 RMS level (95 % measurements for normal error distribution) being ≈ 0.0025 %vol (25 ppm). The relative measurement error does not exceed 0.1 % of the obtained value in the concentration range up to 10 %vol.

A photograph of the developed carbon dioxide sensor prototype is shown in the inset to Fig. 4, *a*. The sensor is a complete industrial-grade device controlled by a microcontroller with digital signal output and high integration of components; it is housed in a compact case of size ⌀20–16 mm and has an average power consumption below 50 mW.

A comparison of the experimental sensor sample characteristics with commercially available analogs showed advantages of the developed sensor in speed (6–30 times), detection threshold (up to 2 times), and dynamic range (more than 2 times) [2,3].

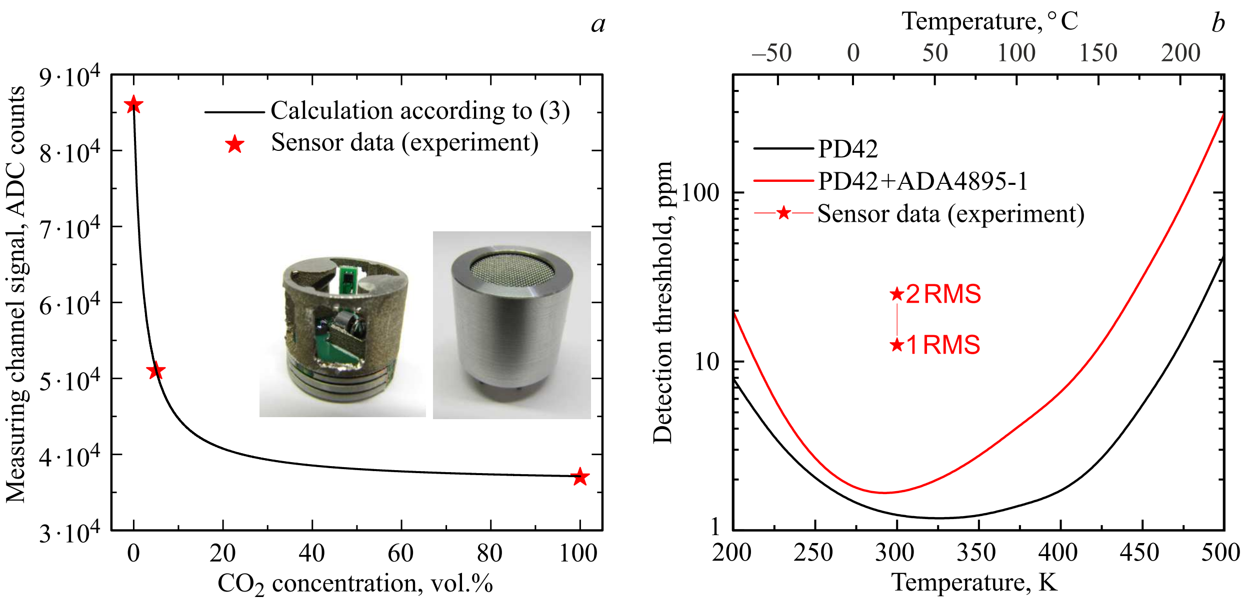

Figure 4. Sensor transfer function at room temperature and prototype photograph (*a*), temperature dependences of detection threshold (*b*).

Conclusion

Light- and photodiodes based on the *n*-InAs/N-InAsSbP/InAsSb/P-InAsSbP heterostructure with an operating wavelength of about 4.2 μm ($T = 296$ K) were obtained and investigated in the temperature range 200–500 K based on which a compact nondispersive carbon dioxide sensor was developed, characterized by a detection threshold of no more than 25 ppm at a sampling frequency of 128 ms, optical path of 2 cm, and power consumption below 50 mW.

Conflict of interest

The authors declare that they have no conflict of interest.

References

[1] E.A. Kochelaev, V.V. Petrov, Optika i spektroskopiya, **131** (10), 1431 (2023). (in Russian). DOI: 10.61011/OS.2023.10.56895.5312-23
[2] Infrakrasnye nedispersionnye gazovye datchiki kompanii Dynament (UK). [Electronic source]. URL: http://www.dynament.ru/pdf/tds0048.pdf
[3] Infrakrasnye nedispersionnye gazovye datchiki kompanii Optosense (RU) [Electronic source]. URL: https://optosense.ru/upload/iblock/212/ESAT.100700.00%20%D0%A0%D0%AD.pdf
[4] N.V. Zotova, N.D. Il'inskaya, S.A. Karandashev, B.A. Matveev, M.A. Remennyj, N.M. Stus', V.V. Shustov, N.G. Tarakanova, FTP, **4** (6), 717 (2006) (in Russian)
[5] A.L. Zakgejm, N.V. Zotova, N.D. Il'inskaya, S.A. Karandashev, B.A. Matveev, M.A. Remennyj, N.M. Stus', A.E. Chernyakov, FTP, **43** (3), 412 (2009). (in Russian)
[6] N.D. Il'inskaya, S.A. Karandashev, N.G. Karpukhina, A.A. Lavrov, B.A. Matveev, M.A. Remennyj, N.M. Stus', A.A. Usikova, FTP, **50** (5), 657 (2016). (in Russian)
[7] S.E. Aleksandrov, G.A. Gavrilov, A.A. Kapralov, B.A. Matveev, M.A. Remennyj, G.Yu. Sotnikova, ZhTF, **88** (9), 1433 (2018). (in Russian) DOI: 10.21883/0000000000
[8] Immersionnye sveto- i fotodiody, rabotayushchie na dline volny 4.2 mkm. [Electronic source]. URL: http://www.ioffeled.com/Specifications/LED42.pdf, URL: http://www.ioffeled.com/Specifications/PD42.pdf
[9] G.A. Gavrilov, B.A. Matveev, G.Yu. Sotnikova, FTP, **37** (18), 50 (2011). (in Russian)

Translated by J.Savelyeva